Materials Science-Poland, 42(1), 2024, pp. 107-115
http://www.materialsscience.pwr.wroc.pl/
DOI: 10.2478/msp-2024-0006

Microstructural, antifungal and photocatalytic activity of NiO–ZnO nanocomposite

Yixuan Wang[1,*] and G. Balakrishnan[2]

[1]School of light Industry, Harbin University of commerce, Harbin, Heilongjiang 150006, China
[2]Saveetha Dental College, Saveetha Institute of Medical and Technical Sciences, Chennai-602105, Tamilnadu, India

In this work, NiO–ZnOnanocomposite (NC)was prepared through a facile, low-temperature,sol–gel route. Zinc acetate dihydrate, nickel chloride hexahydrate, cetyltrimethyl ammonium bromide (CTAB), and citric acid were used in the synthesis of the material. Then, the sample was kept in the muffle furnace at a temperature of 600°C for 2 h. X-ray diffraction (XRD), Fourier transform infrared (FTIR) spectroscopy, field emission scanning electron microscopy (FESEM), UV–Visible spectroscopy, and photocatalytic and antifungal investigations were used to characterize the synthesized nanocrystallites. The XRD data showedthe polycrystalline hexagonal ZnO nanoparticles and cubic NiO crystallites. FTIR studies confirmed the presence of Zn-O and Ni-O bonds in the sample. The FESEM analysis showed the morphology of nanocrystallitescharacterized by their homogeneous shape and size. The absorbance curves from the UV–Visible spectroscopy investigation revealed the bandgap of 3.17 eV. The research findings demonstrate that the NiO–ZnO NC possesses the significant level of selected microbial pathogens. Industrial dyesmake water unhealthy for drinking. Among these dyes, methylene blue (MB) is toxic, carcinogenic, and non-biodegradable, and causes a severe threat to human health and environmental safety. Hence, it is necessary to develop efficient and environmentally friendly technology to remove MB from wastewater. The ZnO–NiO NC degraded the MB dye pollutant under visible irradiation (125 W), according to photocatalytic tests. After 120 min of exposure, the photocatalytic investigations demonstrated 75% degradation efficiency.

Keywords: *antifungal, microstructure, NiO–ZnO-nanocomposite, optical properties, pathogens, photocatalytic*

1. Introduction

The world is currently dealing with two main issues: the growing need for energy and the pollution due to human activity. These are serious issues facing both developed civilizations and developing nations. The textile industries produce a significant amount of organic dyes each year, which has detrimental effects on the environment. Consequently, it is deemed necessary to remove organic dyes from textile wastewater. Additionally, the main sources of pollution are the food, paper, and pharmaceutical sectors, whose effluents affect both surface and ground water. Due to their complex structures, industrial dyes are resistant to the majority of environmental factors that cause degradation [1–4]. As a result, traditional wastewater treatment techniques continue to be inefficient. Organic dyes in wastewater have been eliminated using a wide range of technologies, including membrane filtration, ozonation, adsorption, precipitation, advanced oxidation process (AOP), and biological techniques [5–7]. The adsorption process offers several advantages, including its simplicity in development, cost-effectiveness, ability to recycle the adsorbent, and absence of harmful residue. When contaminated water is exposed to visible light, organic contaminants can be effectively and economically removed through photocatalytic reaction. Due to its potential uses in energy production and environmental protection, semiconductor photocatalysis has garnered a lot of attention in recent decades. Since nanotechnology has advanced, the main focus of photocatalysis research has been on improving the performance and efficiency of already available photocatalysts through adaptation. The photocatalytic activity is attributed to the crystallite forms, sizes, textures, and specific surface areas. Among them, zinc oxide (ZnO) is being researched for numerous uses due to its high electron mobility,

* E-mail: Wa1612720820@outlook.com

© Yixuan Wang and G. Balakrishnan. 2024. This is an open access article distributed under the Creative Commons Attribution-NonCommercial-NoDerivatives 4.0 License. (http://creativecommons.org/licenses/by-nc-nd/4.0/)

and simple- and low-cost synthesis. ZnO typically demonstrates n-type conductivity. However, because of its large bandgap (3.3 eV), ZnO is not a very effective photocatalyst; rapid internal recombination of charge carriers leads to low photo degradation efficiency and impedes the efficient degradation of pollutants. As a result, creating high-performance photocatalysis based on ZnO continues to be difficult [8].

Numerous methods are used to raise ZnO-based photocatalysts' efficiency. It has been observed that doping with metals, non-metals, graphene oxide (GO),and metal oxides improves photocatalytic activity. Coupling ZnO with p-type metal oxides is one efficient way to increase the photocatalytic and antibacterial activities of ZnO. In this case, the heterojunction formation between the n-ZnO and an appropriate p-type can enhance the capacity to use light and enhance the efficiency of photo-generated electron–hole pair separation [9]. NiO, a p-type semiconductor of cubic structure with energy gap of 3.4 e.V, has garnered attention due to its electrical structure, strong hole mobility, and minimum lattice mismatch with ZnO. Consequently, it can be used to create a p–n heterojunction. ZnO's conduction band (CB) is situated between NiO's CB band and the valence band (VB); this arrangement may prevent photo-generated electron–hole pairs from recombining, thereby enhancing photocatalytic efficiency [10].

Microbial resistance is the most complex and complicated problem around the world in medical science. The application of metal-oxide nanoparticlesis one of the most promising strategies to combat microbial resistance to antibiotics. ZnO nanoparticles have demonstrated significant antifungal activity [11]. Because of their enormous surface area, ZnO–NiO nanocomposites (NCs) have been of attention in recent years for use in advanced applications such as gas sensors, solar cells, and antimicrobial properties [12]. This paper presents a method for efficiently breaking down the methylene blue (MB)dye using photocatalysis. The method involves synthesizing the NiO–ZnO composite,utilising the sol–gel technique,with the cetyltrimethyl ammonium bromide (CTAB)capping agent [13].

There are many researchers who have worked on these materials for different applications. Jolaei et al. [14] prepared the pure ZnO, NiO,and ZnO–NiO NCs, which werefound to possess favorable photocatalytic properties. However, it has been observed that ZnO–NiO NCshave a higher photocatalytic efficiency compared to pure ZnO and pure NiO. A sol–gel approach was used to synthesize the ZnO–NiO NC with agrain size of 50 nm. According to antibacterial research, ZnO–NiO NCshave better sensitivity against S. aureus bacteria than against *E. coli*. [11]. Creating heterostructures containing p-type oxides, such as NiO and CuO, is a viable strategy to enhance ZnO's photocatalytic activity. These systems are frequently created using labor-intensive, template-based, growth approaches. Udayachandran Thampy et al. [9] created the ZnO–NiO composite using a sonochemical process that does not require a template. These NCs were then employed to break down MB, an organic dye. Due to its simple and low cost, the sol–gel process is among the finest for creating nanostructures. ZnO and NiO nanoparticles have antibacterial and photocatalytic properties [15–17]. In this study, the NiO–ZnO NC is synthesized through a sol–gel method, and its microstructural,antifungal, and photocatalytic activities are investigated.

2. Materials and methods

The chemicals were purchased from M/s. Sigma Chemicals, USA, for this work. The zinc acetatedihydrate (99%$Zn(CH_3COO)_2.2H_2O$) and then nickel chloride hexahydrate (99.95% $NiCl_2.\ 6H_2O$)were dissolved in DI water separately. These two solutions were mixed together, and then the 0.01 g of CTAB was added as a surfactant and stirred for 30 min. The citric acid was dissolved in DI water and added to the precursor solution dropwise and stirred continuously. The gel was centrifuged five times using DI water and ethanol to remove the impurities. The resultant sample was kept in an oven at 120°C for 24 h for drying and annealed at 600°C for 2 h in a muffle furnace.

Using CuKα radiation, the sample's structure was examined using an X-ray diffractometer

(XRD; Model Smart lab SE X-Ray; Make-Rigaku, Japan). Chemical analysis was performed to verify the chemical bonds using an FTIR spectrometer (Spectrum Two FTIR/ATR spectrometer, Perkin Elmer, USA) in the wavenumber range 400–4000 cm^{-1}. The field emission scanning electron microscope (FESEM) (Carl Zeiss microscopy Ltd, UK & SIGMA) was used to analyze the surface morphology and composition. The absorbance of the sample was measured using a UV-1800, Shimadzu,double-beam spectrophotometer in the 200–1000 nm wavelength range.

2.1. Standard Antibiotics

The standard antibiotic *Flucanazole* was used for this study.

2.1.1. Determination of antifungal activity

In the antifungal activity studies, the pathogenic fungi such as *A. niger, A. flavus, A. fumigatus, and C.albicans, Mucor spp were used.* Utilizing a quantitative microspectrophotometric test, antifungal activity was determined. In 96-well microtiter plates, growth inhibition was assessed at 595 nm. Tests were conducted regularly using 70μL of potato dextrose broth (PDB) (HiMedia, Mumbai, India), 10μL of a spore suspension, and 20μL of the catalyst to be tested. As a negative control, microcultures with 20μL of sterile, distilled water, in place of the test solution, were employed. As a positive control, 0.2 mg/mL of the commercial Fluconazole (FLC 10 mcg SD 114) (2-(2,4-difluorophenyl)-1,3-bis(1H-1,2,4-triazol-1-yl) propan-2-ol) was employed [5]. After allowing the spores to settle for 30 min at 27°C, the absorbance of the plates was measured using an ELISA plate reader at 595 nm. By measuring absorbance, growth was determined following a 48h incubation period at 27°C. Every test for antifungal activity was run in at least three duplicates.

The equation $[(\Delta C–\Delta T)/\Delta C] \times 100$ was used to calculate growth inhibition,

where ΔC represents the corrected absorbance of the control microculture at 595 nm, and ΔT represents the corrected absorbance of the test microculture. The culture's absorbance at 595–nm measured after 48 h, and the absorbance measured after 30min equals the adjusted absorbance values [6].

2.1.2. Minimal inhibitory concentration and minimum fungicidal concentration

With a few minor adjustments, the microplate approach previously reported was utilized to find the lowest inhibitory concentrations (minimal inhibitory concentration [MIC]) of the catalyst. The catalyst wasdiluted, ranging from a 1/2 dilution to a 1/100 dilution. 100μL of each catalyst solution and 100μL of the fungal spore suspension (2×10^6 spores/mL in fresh PDB) were combined in each well. With daily monitoring, the microplates are incubated for2–3 days at 27°C. Every experiment is carried out three times. Using a microplate reader, the MIC measurements are taken at 595 nm. Following a 72 h incubation period, 20μL of each well that doesnot exhibit any visible growth, the last positive well (growth comparable to the growth control well), and the growth control are all sub-cultured onto PDA plates. The growth control subculture showed signs of growth when the plates are incubated at 27°C. The lowest concentration of the catalyst that doesnot result in any fungal growth on the solid medium was considered the minimum fungicidal concentration [7].

2.1.3. Photocatalytic studies

The photo reactor (HEBER, MODELHVAR-MP400) is used to investigate the sample's photocatalytic activity. The visible light (550 nm) with 125 Watts is used for the experiment. Using methylene blue (C16H18CIN3S, Merck) as a model pollutant, the photocatalytic activity of the materials under visible radiation is investigated. A concentration of 10 ppm dye was subjected to stirring, with the addition of 1g/L catalyst. A magnetic stirrer is employed in a continual manner to achieve optimal homogeneity of the solution. The solution is incubated in a dark environment for 30 min to attain adsorption equilibrium, after which the absorbance is measured using a spectrophotometer. The lamp is positioned in the middle of the photoreactor. In the photoreactor, a continuous water flow is implemented to ensure a consistent temperature is

maintained throughout the duration of the experiment.2.5 mL of the solution is taken out at regular intervals of 30 min during the irradiation process to analyze the dye's progress of degradation, with the help of a UV–Visible absorption spectrophotometer. The dye's as-prepared absorption spectra served as a control for calculating the percentage of degradation. The intensity of MB's 664 nm absorption peak is analyzed to track the development of the dye degradation reaction. The absorption of the material is calculated from the formula

$$\boxed{\text{Degradation } \% \ = \ (C_o - C)/C_o \times 100\%,}$$

where C_o and C are the initial and final concentrations of the dye and the absorption capacity of a specific catalyst is calculated using

$$\boxed{Q = (C_o - C)\ V/m}$$

V – volume of the solution; m – mass of the catalyst.

3. Results and Discussion

3.1. X-ray diffraction (XRD) analysis

With the use of XRD pattern (Figure 1),theNC's crystal structure is identified. The peaks at angles 37.1°, 43.1°, 62.5°, 75.0°, and 78.9° denote the (111), (200), (220), (311), and (222) planes of NiO(JCPDS # 04-0835), respectively, which belong to the FCC structure of NiO, and, also,the relative intensities of the distinctive peaks are in accordance with the standard pattern. The peaks are also visible at angles 31.7°, 34.44°, 36.2°, 47.5°, 51.8°, 56.5°, 67.8°, 69.0°, and 76.2° in the XRD pattern. These peaks correspond to (100), (002), (101), (100), (102), (110), (200), (201), (112), and (202) reflections, respectively, which denote the ZnO hexagonal structure (JCPDS # 89-1397). The peaks from cubic NiO and hexagonal ZnO are evident in the NiO–ZnO NC sample. For ZnO and NiO NC, no further impurity peaks are seen, and the distinct peaks shown in the XRD pattern attest to the development of highly polycrystalline ZnO and NiO phases. The crystallite size is computed using the Scherer's formula.

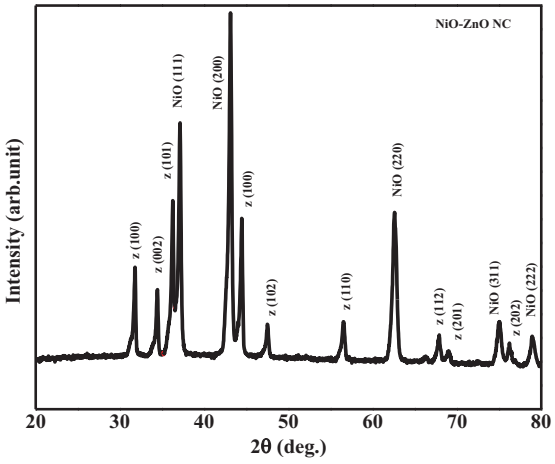

Fig. 1. X-ray diffraction pattern of NiO–ZnO NC. NC, nanocomposite

The (101) reflection of ZnO is used to calculate the crystallite sizeand is found to be 39 nm, while crystallite size of NiO is 23 nm, calculated from the (200) peak of NiO. The results obtained in this work are consistent with the results of Jolaei et al. [14]. The ZnO–NiO NCsare synthesized using the co-precipitation method, and the crystalline structure of ZnO is confirmed as hexagonal (JCPDS File No. 80-0075), while the structure of NiO is cubic (JCPDS File No. 78-0429). The synthesis of the NiO–ZnO NC photocatalyst is achieved by co-precipitation and co-gel formation processes [18]. The XRD pattern exhibit reflections correspond to both pure NiO and ZnO.

3.2. FTIR spectroscopy analysis

The bands corresponding to 416, 1,946, 2,004, 2,025, 2,075, 2,202, 2,181, 2,235, and 3,650 cm^{-1} are obtained from Fourier transform infrared (FTIR) spectroscopy investigation of NiO–ZnO NC. The peak observed at 2,000–2,235 cm^{-1} represents the adsorption of ambient CO_2 on the surface of the NC. Figure 2 demonstrates that the hydroxyl group's stretching vibration is seen in the transmittance band in the 3650 cm^{-1} range. The peaks at 1946 cm^{-1} can be attributed to the bending vibration of the OH bond. Nickel and zinc metal oxides can be seen at the maxima at 455 cm^{-1} and 416 cm^{-1}, respectively [19].

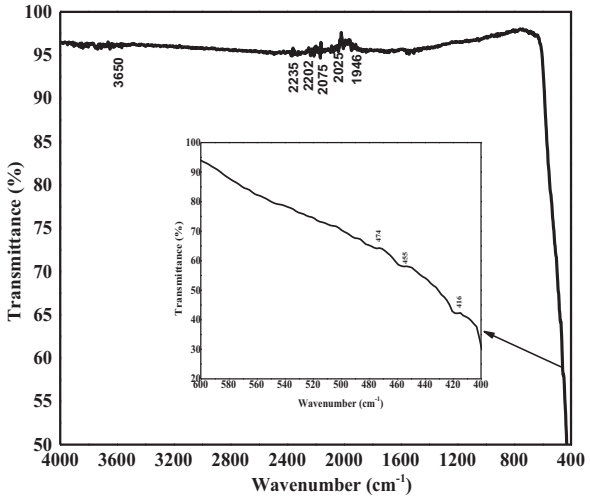

Fig. 2. FTIR spectrum of NiO–ZnO NC

3.3. Field emission-scanning electron microscopy (FE-SEM) analysis

FESEM is a powerful technique to analyze the surface topography and crystallite size. Figures 3A–3D shows the NiO–ZnONC with different magnifications. The micrographs show formation of crystallites with uniform size with dense structure. The dense structure isformed with specific shape and size. The EDS results are shown in Figure3E, which reveals the Zn, Ni, and oxygen elements, indicating the presence of ZnO and NiO,with no impurities. Thenickel, zinc, and oxygen, ascertained using EDX analysis, are 9.71%, 39.34%, and 50.95%, (wt%),respectively. The EDX results are determined to be similar to the findings reported by Karthikeyan et al. [12] and Haq et al. [19].

3.4. UV–Visible Spectroscopy Analysis

The absorbance spectra of the NiO–ZnO NC, obtained in the 200–1,000 nm region, are displayed in Figure 4. The sudden absorbance indicates the bandgap of the material. The interaction between the incident photon and the substance has enough energy when the wavelength is smaller, which causes the absorbance to rise. The spectrum shows the absorbance to be about 390 nm. The approximate bandgap can be calculated by means of the equation E (eV) = 1,240/Wavelength (nm) = 3.17 eV. The bandgap of the NiO–ZnO NC is found to be ∼3.17e.V, and this value is comparable with the other reported results. Weldekirstos et al. [13] calculated the bandgap using the Tauc plot and found the value of 2.90 eV. Jolaei et al. [14] calculated the optical bandgap of ZnO–NiO NC,and the value is found to be 2.94 eV.

3.5. Antifungal activity studies

The majority of tribal residents frequently suffer from infectious diseases, especially skin and mucosal infections, as a result of poor sanitation, unclean drinking water, and a lack of knowledge about healthy eating practices. Among these skin pathogens, fungus play a significant role. Notable species include Candida spp. and dermatophytes. In the case of *A. niger* (Table 1), at the drug concentration between 250 μg/mL and 1000 μg/mL, the zone of inhibition for *flucanazole* was 10 mm, whereas the NC had 10, 10, 11, and 12 mm. In *A.flavus*, for the drug concentration between 250 μg/mL and 1000μg/mL, the zone of inhibition was 10 mm in *flucanazole* and 11.4–14 mm range for the NC. In the case of *A.fumigatus* at the drug concentration between 250 μg/mL and 1000 μg/mL, the zone of inhibition for *flucanazole* was 8.0 mm and 8 mm, 9 mm, 9 mm, 10 mm for NC. In the case of *C. albicans*, it was 10 mm in *flucanazole*, whereas the NC gave 11, 12, 12, and 13 mm for different concentrations. In *Mucorspp*, at the drug concentration between 250 μg/mL and 1000μg/mL, the zone of inhibition for *flucanazole* was 10 mm, whereas for the NC, it was 10.2, 10.8, 11, and 12 mm. The present work clearly indicates that the NiO–ZnO NC possesses significant antifungal activity against pathogenic fungi such as *A.niger, A.flavus, A.fumigatus, C.albicans, and Mucorspp*. Hussein et al. [11] examined the antibacterial properties of NiO–ZnO NCagainst both Gram-positive (G + Ve) bacteria–specifically, S. aureus, and Gram-negative (G-Ve) bacteria–specifically *E. coli*. The results indicated that the antibacterial activity of the NC was more pronounced against S. aureus compared to *E. coli*.

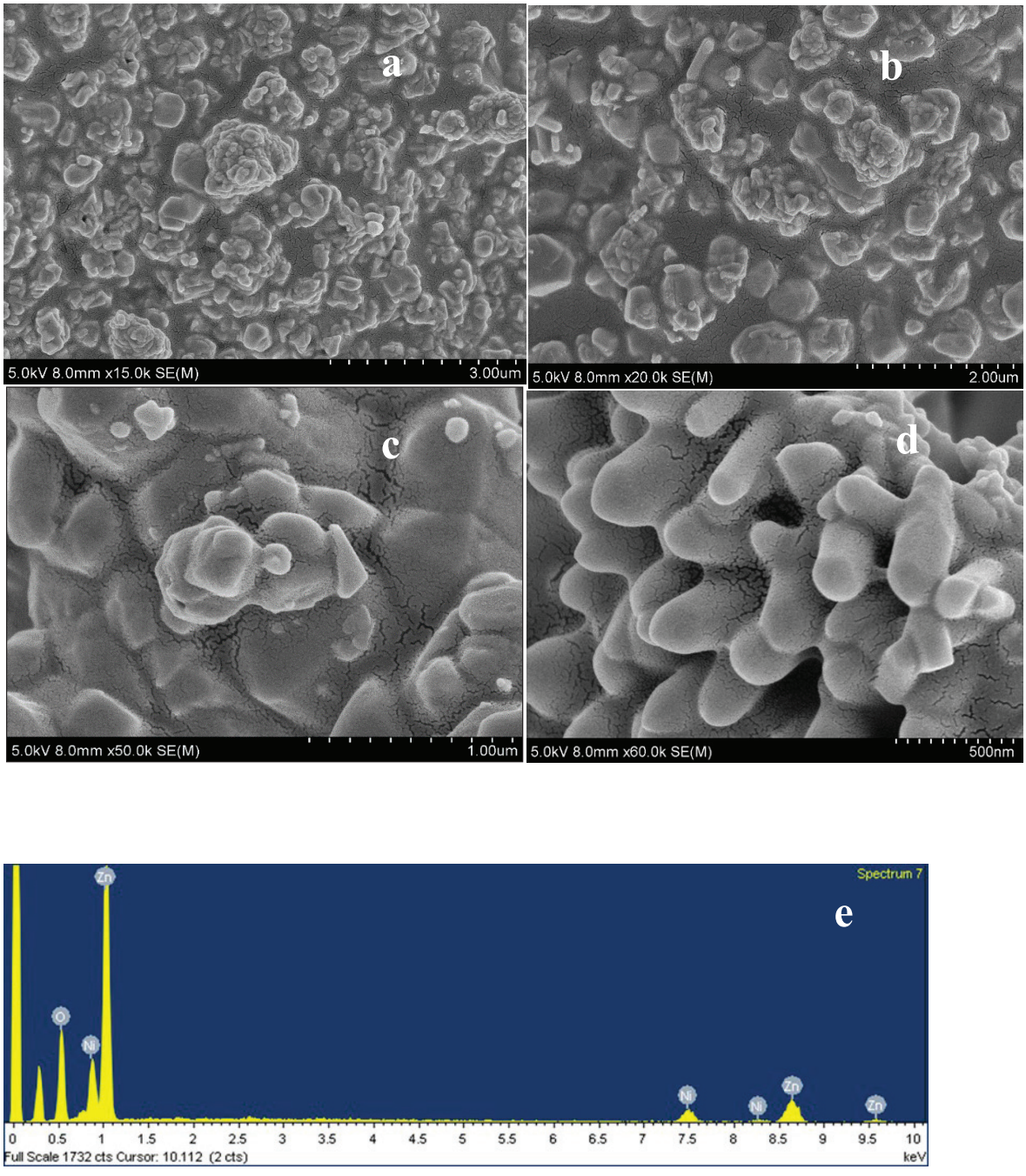

Fig. 3. **(A–D)** FE-SEM micrographs of NiO–ZnO NC with different magnifications (15, 20, 50 and 60 K) and **(E)** EDX spectrum. NC, nanocomposite

3.6. Photocatalytic activity studies

Nanoparticlessuch as photocatalystshave significant potential for environmental friendly removal of major pollutants such as organic dyes, heavy metals, and pesticides from industrial waste. Figure 5 depicts the process of photo degradation of MB dye using ZnO–NiO as a catalyst. The studies were conducted to assess the impact of a catalyst on MB dye degradation using visible radiation. The graph illustrates the highest level of intensity reached by the MB dye

Table 1. Shows that MIC of flucanazole and NiO–ZnO NC

S.No	Test organism/Fungai	Zone of inhibition (mm)				
		Standard	**250 μg**	**500 μg**	**750 μg**	**1,000 μg**
1	*A. niger*(E)	10 ± 1.00	12 ± 1.10	14 ± 1.20	15.5 ± 1.20	17 ± 1.30
2	*A. flavus*(D)	10 ± 0.8	12.4 ± 1.0	15 ± 1.10	16.0 ± 1.2	18 ± 1.2
3	*A.fumigatus*(C)	8 ± 0.6	10.0 ± 0.8	11.5 ± 1.0	13 ± 1.1	14 ± 1.2
4	*C. albicans* (B)	10 ± 0.9	12 ± 1.0	14 ± 1.1	15.5 ± 1.2	17 ± 1.2
5	*Mucor sp.*(A)	10 ± 0.8	12.5 ± 1.0	14.5 ± 1.2	16 ± 1.3	17 ± 1.4

MIC, minimal inhibitory concentration; NC, nanocomposite.

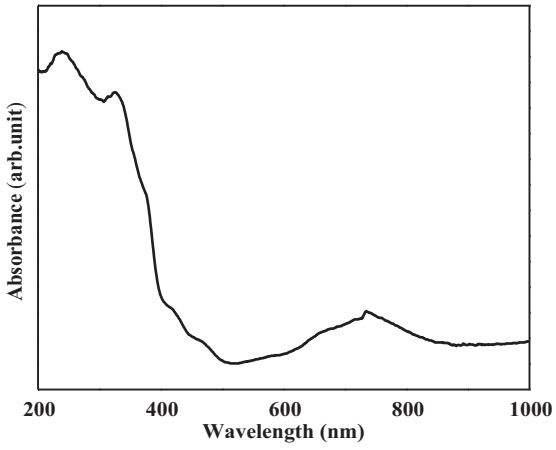

Fig. 4. Absorbance spectrum of NiO–ZnO NC. NC, nanocomposite

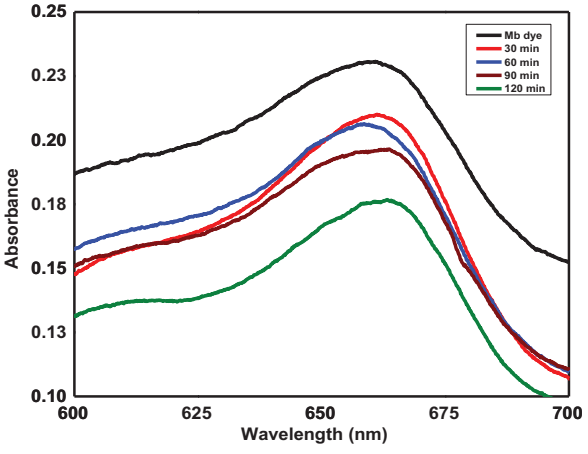

Fig. 5. Photocatalytic degradation of MB dye using ZnO/NiO catalyst. MB, methylene blue

under dark conditions. Over time, the intensity of absorbance for the MB dye diminishes. The rate of a chemical reaction can be altered by exposing it to specific wavelengths of ultraviolet, visible, and infrared light energy. The catalyst absorbs this energy, leading to the generation of electron–hole pairs (e–h). These pairs then generate highly reactive reducing and/or oxidizing radicals on the conduction and valence bands, respectively. The radicals present in contaminated water undergo secondary reactions to destroy both organic and inorganic pollutants. After a duration of 120 min, the absorbance reaches its lowest point, and the MB dye solution loses its color, showing the breakdown of the pollutant due to radiation. The catalyst exhibited a consistent and proportional rise in the absorption of MB when exposed to visible light.

Paul et al. [20] synthesized NiO–ZnO NC and analyzed the photocatalytic activity. The photocatalytic reduction of MB exhibited kinetics,indicating the homogeneous adsorption of MB on the NC's surface. Udayachandran Thampy et al. [9] studied the photocatalytic property of ZnO–NiO NC in breaking down MB dye using sun irradiation. The researchers found that the NC exhibited a much superior photocatalytic performance in comparison to pure ZnO and NiO. The enhanced photocatalytic performance of the composite can be ascribed to the improved separation of charge carriers, facilitated by the internal electric field at the interface of ZnO and NiO. The evaluation of the photocatalytic efficiency of NiO–ZnO NC was conducted by quantifying the degradation of MB dye under a continuous stream of visible radiation [15]. The synthesized ZnO nanoparticles had the capacity to degrade the MB dye by up to 76% at the specified conditions. The transition from a rich blue color to a colorless state can be visibly observed as a result of the breakdown

of the MB dye when exposed to radiation. NiO–ZnO NC was prepared using a microwave-assisted approach,and the subsequent experiment utilized a prearranged NC to facilitate the photodegradation of MBdye and Rhodamin B when exposed to UV light [21]. Almost all the researchers used only UV light for the photocatalytic degradation, while the present work utilized the visible light for the photocatalytic degradation,and the work demonstrated that the NC exhibits exceptional photocatalytic efficacy of 75%.

4. Conclusions

Sol–gel method was used to prepare the NiO–ZnO NC,and the microstructural, optical, photocatalytic, and antifungal properties were investigated. XRD analyses revealed that the NiO possessesa cubic phase, while ZnO showed a polycrystalline, hexagonal structure. The crystallite sizeswere computed for ZnO and NiO, and were found to be 39 nm and 23 nm, respectively. The formation of Ni-O and Zn-O bonds was confirmed using FTIR measurements. The FESEM results provided evidence of the successful formation of crystalliteswith a uniform size and compact structure. The 3.17 eV bandgap was obtained via UV–Visible spectroscopy studies. The antifungal studies showed that the ZnO–NiONC indicated good sensitivity against fungi. According to photocatalytic experiments, when exposed to visible light, the NCsbreakdown the MB dye pollutant. After exposure to radiation for 120 min, the NCs' deterioration efficiency was approximately 75%.

References

[1] Malato S, Fernandez-Ibanez P, Maldonado MI, Blanco J, Gernjak W. Decontamination and disinfection of water by solar photocatalysis: recent overview and trends. *Catal Today*. 2009;147: 1–59.

[2] Chong MN, Jin B, Chow CWK, Saint C. Recent developments in photocatalytic water treatment technology: areview. *Water Res*. 2010;44:2997–3027.

[3] Bodzek M, Rajca M. Photocatalysis in the treatment and disinfection of water. Part I. Theoretical backgrounds. *Ecol Chem Eng S*. 2012;19(4):489–512.

[4] Mishra S, Sundaram B. A review of the photocatalysis process used for wastewater treatment. In: *Materials Today: Proceedings*, 2023; doi: 10.1016/j.matpr.2023.07.147

[5] Davies J, Davies D. Origins and evolution of antibiotic resistance. *Microbiol Mol Biol Rev*. 2010;74(3): 417–33.

[6] Cavalieri F, Tortora M, Stringaro A, Colone M, Baldassarri L. Nanomedicines for antimicrobial interventions. *J Hosp Infect*. 2014;88(4): 183–90.

[7] Reygaert W. An overview of the antimicrobial resistance mechanisms of bacteria. *AIMS Microbiol*. 2018;4(3):482–501.

[8] Ong CB, Ng LY, Mohammad AW. A review of ZnO nanoparticles as solar photocatalysts: synthesis, mechanisms, and applications. *Renew Sust Energ Rev*. 2018;81: 536–51.

[9] Udayachandran Thampy US, Mahesh A, Sibi KS, Jawahar IN, Biju V. Enhanced photocatalytic activity of ZnO–NiO nanocomposites, synthesized through a facile sonochemical route. *SN Appl Sci*. 2019;1: 1478.

[10] Mirzaeifard Z, Shariatinia Z, Jourshabani M, Darvishi SMR. ZnO photocatalyst revisited: effective photocatalytic degradation of emerging contaminants using S-doped ZnO nanoparticles under visible light radiation. *Ind Eng Chem Res*. 2020;59: 15894–911.

[11] Hussein IF, Nusseif AD, Majeed AMA. Analytical study of ZnO:NiO nanocomposite of antibacterial activities. *Plant Archives*. 2020;20: 2747–50.

[12] Karthikeyan V, Padmanaban A, Dhanasekaran T. Synthesis and characterization of ZnO:NiO and its photocatalytic activity. *Mech Mater Sci Eng J*.2017;10: 95–99. doi: 10.2412/mmse.23.8.292

[13] Weldekirstos HD, Habtewold B, Kabtamu DM. Surfactant-assisted synthesis of NiO-ZnO and NiO-CuO nanocomposites for enhanced photocatalytic degradation of methylene blue under UV light irradiation. *Front Mater*. 2022;9: 832439.

[14] Jolaei S, Mirzaei M, Hassanpour A, Safardoust-Hojaghan H, Khani A. Using ZnO, NiO, and ZnO/NiO as nano photocatalysts for removal of acid violet and rhodamine B from wastewater. *J Nanostruct*. 2022;12(3):761–70.

[15] Sajjad B, Ali S, Farrukh AM. Synthesis of NiO/ZnO nanoparticles: application for photodegradation of methylene blue. *J Sci Comput Eng Res*. 2020: 95–9.

[16] Poliukhova V, Cho SH, Orlov A. ZnO–NiO composites for photocatalysis of methylene blue. In: *2018 IEEE 38th International Conference on Electronics and Nanotechnology (ELNANO)*, Kyiv, Ukraine; 2018. p. 191–6.

[17] Kerli S, Alver Ü. Preparation and characterisation of ZnO/NiO nanocomposite for solar cell applications. *J Nanotechnol*. 2016: Article ID 4028062, 5 pages.

[18] Hameed A, Montini T, Gombac V, FornasieroP. Photocatalytic decolourization of dyes on NiO–ZnO nanocomposites. *Photochem Photobiol Sci*. 2009;8: 677–82.

[19] Haq S, Raja AW, Rehman SU, Mezni A, Ali MB, Hedfi A, et al. Phytogenic synthesis and characterization of NiO-ZnO nanocomposite for the photodegradation of brilliant green and 4-nitrophenol. *J Chem*. 2021: Article ID 3475036. doi: 10.1155/2021/3475036

[20] Paul D, Maiti S, Sethi DP, NeogiS. Bi-functional NiO–ZnO nanocomposite: synthesis, characterization, antibacterial and photo-assisteddegradation study. *Adv Powder Technol*. 2021;32: 131–43.

[21] Hassanpour M, Safardoust-Hojaghan H, Salavati-NiasariM. Rapid and eco-friendly synthesis of NiO/ZnO nanocomposite and its application in decolorization of dye. *J Mater Sci: MaterElectron*. 2017;28: 10830–7.

Received 2023-12-28
Accepted 2024-04-11